

# Stoichiometry and Subunit Arrangement of $\alpha 1\beta$ Glycine Receptors As Determined by Atomic Force Microscopy

Zhe Yang,<sup>†</sup> Elena Taran,<sup>‡</sup> Timothy I. Webb,<sup>†</sup> and Joseph W. Lynch<sup>\*,†,§</sup>

<sup>†</sup>Queensland Brain Institute, <sup>‡</sup>Australian Institute for Bioengineering and Nanotechnology, Australian National Fabrication Facility Queensland Node, and <sup>§</sup>School of Biomedical Sciences, University of Queensland, Brisbane, QLD 4072, Australia

## Supporting Information

**ABSTRACT:** The glycine receptor is an anion-permeable member of the Cys-loop ion channel receptor family. Synaptic glycine receptors predominantly comprise pentameric  $\alpha 1\beta$  subunit heteromers. To date, attempts to define the subunit stoichiometry and arrangement of these receptors have not yielded consistent results. Here we introduced FLAG and six-His epitopes into  $\alpha 1$  and  $\beta$  subunits, respectively, and imaged single antibody-bound  $\alpha 1\beta$  receptors using atomic force microscopy. This permitted us to infer the number and relative locations of the respective subunits in functional pentamers. Our results indicate an invariant  $2\alpha 1:3\beta$  stoichiometry with a  $\beta-\alpha-\beta-\alpha-\beta$  subunit arrangement.

Glycine receptor (GlyR) chloride channels mediate inhibitory transmission in the spinal cord and brain stem.<sup>1</sup> As they are considered potential therapeutic targets for indications including inflammatory pain, hyperekplexia, spasticity, tinnitus, and breathing disorders,<sup>2–5</sup> there is widespread interest in the molecular structure of their ligand binding sites for therapeutic development. GlyRs are members of the pentameric Cys-loop ion channel receptor family. Because ligand-binding sites are located at subunit interfaces, the pharmacological properties of each binding site are defined by the contributing subunits.<sup>6</sup> It is thus of interest to establish the subunit stoichiometry and arrangement in functional receptors to determine the number and type of subunit interfaces. Synaptic GlyRs are  $\alpha\beta$  heteromers, and receptors resulting from the cotransfection of varying amounts of  $\alpha$  and  $\beta$  subunit RNA have uniform functional properties, implying a fixed stoichiometry.<sup>7,8</sup> Depending on their stoichiometry, heteromeric GlyRs may contain a mixture of  $\alpha-\alpha$ ,  $\alpha-\beta$ ,  $\beta-\alpha$ , and  $\beta-\beta$  interfaces.

The initial characterization of affinity-purified native GlyRs inferred that heteromeric GlyRs comprised  $3\alpha$  and  $2\beta$  subunits.<sup>9,10</sup> This stoichiometry was supported by a subsequent functional analysis that showed the effect of a pore mutation was more dramatic when it was inserted into the  $\alpha$  relative to the  $\beta$  subunit, implying an excess of  $\alpha$  subunits per pentamer.<sup>11</sup> However, a study that compared the effects of mutations to corresponding glycine binding residues in  $\alpha 1$  and  $\beta$  subunits concluded that  $\beta$  subunits predominated in  $\alpha 1\beta$  GlyRs.<sup>12</sup> They then showed that  $\alpha 1\beta$  concatemers produced functional heteromers when coexpressed with  $\beta$  monomers but not when expressed alone or with  $\alpha 1$  monomers. This was

consistent with either a  $2\alpha:3\beta$  or a  $1\alpha:4\beta$  stoichiometry. Quantitation of radiolabeled methionine levels in recombinant  $\alpha 1$  and  $\alpha 1\beta$  GlyRs allowed the authors to deduce a  $2\alpha 1:3\beta$  stoichiometry, with a  $\beta-\alpha-\beta-\alpha-\beta$  arrangement.<sup>12</sup>

However, potential problems with using concatemers include dimer proteolysis,<sup>13</sup> dipentamer formation,<sup>14</sup> and incomplete incorporation of fusion protein into individual pentamers.<sup>15</sup> These problems are more likely to occur when dimers are cotransfected with monomers than when fully concatenated pentamers are used.<sup>16,17</sup> Thus, as the GlyR dimer experiments<sup>12</sup> may not be definitive, alternate approaches to confirming the subunit stoichiometry and arrangement are warranted. For this reason, we probed the subunit arrangement of  $\alpha 1\beta$  GlyRs using atomic force microscopy (AFM), using a previously described methodology.<sup>18,19</sup>

FLAG and six-His epitopes were added to  $\alpha 1$  and  $\beta$  subunits, resulting in subunits that we term  $\alpha 1_{\text{flag}}$  and  $\beta_{6\text{his}}$  (Supporting Information). The functional expression of  $\alpha 1_{\text{flag}}\beta_{6\text{his}}$  GlyRs was verified by electrophysiology. Robust whole-cell currents activated by saturating (3 mM) and EC<sub>20</sub> (30  $\mu\text{M}$ ) glycine concentrations were seen in cells transfected with  $\alpha 1_{\text{flag}}$  subunits or  $\alpha 1_{\text{flag}}$  and  $\beta_{6\text{his}}$  subunits in a 1:1 ratio (Figure 1A). To confirm the successful incorporation of  $\beta_{6\text{his}}$  subunits

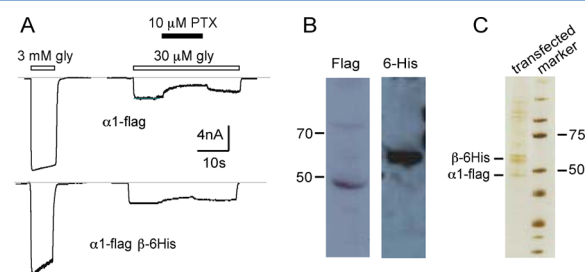


**Figure 1.** Functional expression and immunoblot analysis of  $\alpha 1_{\text{flag}}$  and  $\beta_{6\text{his}}$  GlyRs. (A) Electrophysiological recordings from HEK293 cells transfected with  $\alpha 1_{\text{flag}}$  DNA (top) and  $\alpha 1_{\text{flag}}$  and  $\beta_{6\text{his}}$  DNA (bottom) at indicated glycine and picrotoxin concentrations. Scale bars apply to all traces. (B) Western blots of  $\alpha 1_{\text{flag}}\beta_{6\text{his}}$  GlyR protein probed with FLAG (left) and six-His antibodies (right). (C) Silver-stained gel of the protein isolated from HEK293 cells transfected with  $\alpha 1_{\text{flag}}$  and  $\beta_{6\text{his}}$  DNA. Size markers are shown (numbers in kilodaltons).

Received: January 16, 2012

Revised: June 6, 2012

Published: June 20, 2012

into GlyR heteromers, the effects of 10  $\mu\text{M}$  picrotoxin on currents activated by 30  $\mu\text{M}$  glycine were quantitated. Picrotoxin inhibited the  $\alpha 1_{\text{flag}}$  homomeric and  $\alpha 1_{\text{flag}}\beta_{6\text{his}}$  heteromeric GlyRs by  $76 \pm 5\%$  ( $n = 6$ ) and  $19 \pm 1\%$  ( $n = 5$ ), respectively (e.g., Figure 1A). This difference was statistically significant ( $P < 0.01$  by unpaired  $t$  test). Given that  $\beta$  subunits confer resistance to picrotoxin inhibition, this demonstrates the efficient incorporation of  $\beta_{6\text{his}}$  subunits into functional heteromers.

Heteromeric  $\alpha 1_{\text{flag}}\beta_{6\text{his}}$  GlyR protein was purified from crude membrane fractions on a  $\text{Ni}^{2+}$ -agarose column via  $\beta$  subunit six-His tags. The  $\alpha 1_{\text{flag}}$  and  $\beta_{6\text{his}}$  subunits have molecular masses of 49 and 59 kDa, respectively, allowing for the tags. Figure 1B demonstrates bands of appropriate size on Western blots probed with FLAG or six-His antibodies. A silver-stained gel of  $\alpha 1_{\text{flag}}\beta_{6\text{his}}$  protein demonstrates a high degree of purity but reveals two bands at 59 kDa (Figure 1C). Because both bands exhibit immunoreactivity with an anti-myc antibody (Figure S1 of the Supporting Information), we infer that they represent full-length and cleaved  $\beta_{6\text{his}}$  subunits. Proteins producing the nonspecific bands are unlikely to assemble into pentamers that are the same size as  $\alpha 1\beta$  GlyRs and should thus be readily excluded from AFM analysis.

Solubilized heteromeric protein samples were plated onto mica chips for AFM imaging. As shown in Figure 2A, the

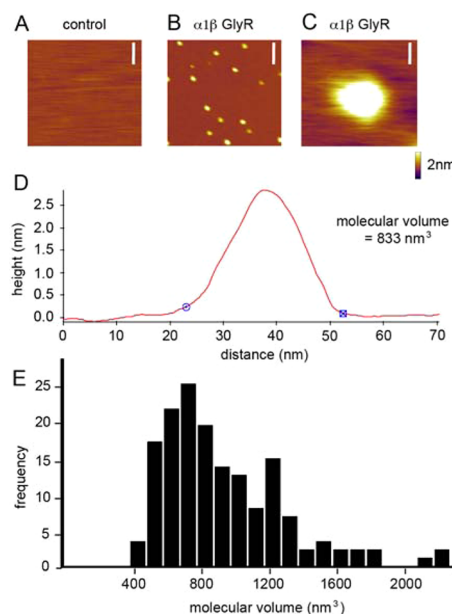


**Figure 2.** AFM imaging of heteromeric GlyRs. (A) Negative control using a sample prepared from mock transfected cells. The scale bar is 100 nm. (B) Low-magnification image of  $\alpha 1\beta_{6\text{his}}$  GlyRs. The scale bar is 200 nm. (C) High-magnification image of a single unlabeled  $\alpha 1_{\text{flag}}\beta_{6\text{his}}$  receptor. The scale bar is 10 nm. (D) Cross section (along the red line) through the receptor imaged in panel C together with its calculated volume. This receptor exhibited a height of 2.6 nm and a radius at half-height of 14.5 nm. (E) Frequency distribution of 139 receptor volumes.

sample prepared from mock transfected cells yielded few, if any, particles. However, the sample from cells expressing recombinant heteromeric GlyRs yielded particles of a predominantly uniform size (Figure 2B). A higher-magnification view of a single large particle is shown in Figure 2C, with a cross section through it shown in Figure 2D. The molecular volumes of the

large particles were calculated from their heights and mean radii at half-height. The measured molecular volume was calculated using the equation<sup>19</sup>  $V_m = (\pi h/6)(3r^2 + h^2)$ , where  $h$  is the height and  $r$  is the radius at half-height. The frequency distribution of measured molecular volumes of 139 large particles yielded a median size of 802  $\text{nm}^3$  (Figure 2E). The theoretical molecular volume of a heteromeric GlyR was calculated using the equation<sup>19</sup>  $V_c = (M_0/N_0)(V_1 + dV_2)$ , where  $M_0$  is the molecular mass,  $N_0$  is Avogadro's number,  $V_1$  and  $V_2$  are the partial specific volumes of the particle and water, respectively, and  $d$  is the extent of protein hydration. Inserting values for protein ( $V_1 = 0.74 \text{ cm}^3/\text{g}$ ) and water ( $V_2 = 1 \text{ cm}^3/\text{g}$ ) only and assuming  $d = 0.4 \text{ cm}^3/\text{g}$  of protein,<sup>18</sup> we calculated a molecular volume of 536  $\text{nm}^3$ . Thus, the measured volume was 50% larger than predicted. A similar overestimation (48%), which was attributed to the binding of detergent to the transmembrane domains, was reported for 5-HT<sub>3</sub> Cys-loop receptors.<sup>18</sup> We thus conclude that the large particles represent individual pentameric GlyRs. The "tail" of higher volumes in Figure 2E has previously been observed in similar Cys-loop receptor AFM studies<sup>18,19</sup> and most likely represents high-molecular mass protein aggregates. An assessment of predicted antibody size is provided in the Supporting Information.

Sample images of  $\alpha 1_{\text{flag}}\beta_{6\text{his}}$  GlyRs and FLAG or six-His antibodies plated alone or following co-incubation of the receptor with the antibody are shown in panels A and B of Figure 3. We observed one or more antibodies in close

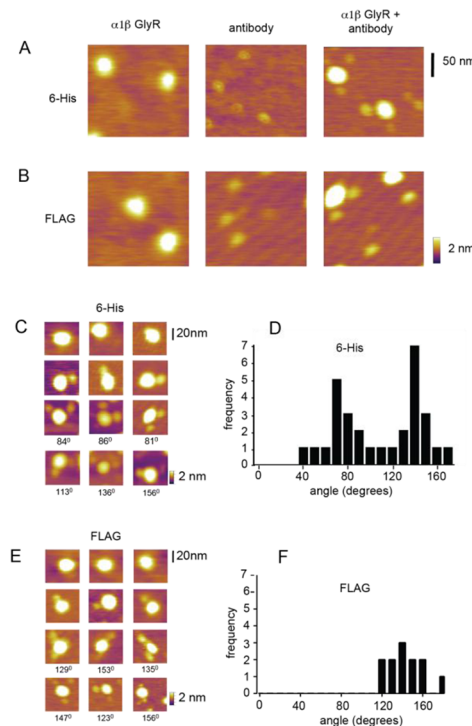


**Figure 3.** AFM imaging of complexes between  $\alpha 1_{\text{flag}}\beta_{6\text{his}}$  GlyRs and six-His or FLAG antibodies. (A) Image of  $\alpha 1_{\text{flag}}\beta_{6\text{his}}$  GlyR protein only, six-His antibody only, and  $\alpha 1_{\text{flag}}\beta_{6\text{his}}$  GlyR and the antibody together. (B) Image of  $\alpha 1_{\text{flag}}\beta_{6\text{his}}$  GlyR protein only, FLAG antibody only, and  $\alpha 1_{\text{flag}}\beta_{6\text{his}}$  GlyR and the antibody together. (C) Sample images showing zero, one, and two six-His antibodies bound to  $\alpha 1_{\text{flag}}\beta_{6\text{his}}$  GlyRs. (D) Frequency histogram of six-His antibody labeling showing peaks near  $72^\circ$  and  $144^\circ$ . (E) Sample images showing zero, one, and two FLAG antibodies bound to  $\alpha 1_{\text{flag}}\beta_{6\text{his}}$  GlyRs. (F) Frequency histogram of FLAG antibody labeling showing a single peak near  $144^\circ$ .

association with only a minority of receptors. Criteria for determining the attachment of an antibody to receptors are described in the Supporting Information. With the six-His antibody, we observed 63 single, 30 double, and 3 triple attachments in a total of ~500 imaged receptors. With the FLAG antibody, we observed 105 single, 12 double, and no triple attachments in ~800 receptors. We never observed more than three antibodies attached to a single receptor. In control experiments, we never saw attachments of the FLAG antibody to GlyR protein that did not express FLAG tags (not shown). Figure 3C shows sample images with zero, one, or two six-His antibody attachments per receptor. In the case of double attachments, the frequency distribution of all angles is shown in Figure 3D. Theoretically, antibodies attached to adjacent and nonadjacent subunits in a pentamer should subtend angles of 72° and 144°, respectively. The existence of maxima at both angles suggests that  $\beta$  subunits may reside adjacent or opposite to each other in pentameric oligomers. In contrast, the angles subtended by FLAG antibodies were invariably clustered near 144° (Figure 3E,F), suggesting  $\alpha$ 1 subunits cannot exist side by side. Results from panels D and F of Figure 3 indicate that  $\alpha$ 1 $\beta$  GlyRs exist in an invariant  $\beta$ - $\alpha$ - $\beta$ - $\alpha$ - $\beta$  arrangement.

This agrees with the previous study that employed tandem concatemers.<sup>12</sup> It was, however, prudent to confirm the stoichiometry for three main reasons. First, as noted above, determination of Cys-loop receptor stoichiometry using combinations of dimers and monomers is not always reliable.<sup>16,17</sup> Second, other evidence also exists in favor of a 3 $\alpha$ :2 $\beta$  stoichiometry.<sup>9,11</sup> The third reason relates to the finding that glycine-mediated conformational changes in GlyRs are transmitted to the channel gate via  $\alpha$  subunits only.<sup>20</sup> It would be surprising that, despite  $\beta$  subunits predominating numerically in  $\alpha$ 1 $\beta$  GlyRs, they have no role in channel activation.

A limitation of AFM is that it cannot differentiate between functional and nonfunctional pentameric constructs, and it is possible that our protein purification procedure preferentially isolated nonfunctional receptors. Indeed, such an explanation has recently been proposed to explain the mismatch in stoichiometries of heteromeric 5-HT<sub>3</sub> receptors as inferred by functional analysis<sup>21,22</sup> and AFM.<sup>18</sup> However, given that we purified membrane-expressed receptors and our tagged constructs produced robust glycine-activated currents, it is unlikely that we exclusively imaged a nonfunctional receptor population. In conclusion, our results support an invariant 2 $\alpha$ 1:3 $\beta$  stoichiometry with a  $\beta$ - $\alpha$ - $\beta$ - $\alpha$ - $\beta$  arrangement. This should help resolve the uncertainty that currently exists concerning the modeling of subunit interface drug binding sites and the interpretation of site-directed mutagenesis data from  $\alpha$ 1 $\beta$  GlyRs.

## ■ ASSOCIATED CONTENT

### ■ Supporting Information

Methods. This material is available free of charge via the Internet at <http://pubs.acs.org>.

## ■ AUTHOR INFORMATION

### Corresponding Author

\*Phone: +61733466375. E-mail: [j.lynch@uq.edu.au](mailto:j.lynch@uq.edu.au).

### Author Contributions

Z.Y., T.I.W., and J.W.L. conceived and designed the experiments. Z.Y., T.I.W., and E.T. conducted experiments and analyzed data.

## Funding

This research was funded by the NHMRC.

## Notes

The authors declare no competing financial interest.

## ■ ACKNOWLEDGMENTS

We thank Prudence Donovan for help with protein purification and Dr. Rick Webb for help with electron microscopy experiments to optimize the protein dispersal conditions.

## ■ REFERENCES

- (1) Lynch, J. W. (2009) *Neuropharmacology* 56, 303–309.
- (2) Chung, S. K., Vanbellinghen, J. F., Mullins, J. G., Robinson, A., Hantke, J., Hammond, C. L., Gilbert, D. F., Freilinger, M., Ryan, M., Kruer, M. C., Masri, A., Gurses, C., Ferrie, C., Harvey, K., Shiang, R., Christodoulou, J., Andermann, F., Andermann, E., Thomas, R. H., Harvey, R. J., Lynch, J. W., and Rees, M. I. (2010) *J. Neurosci.* 30, 9612–9620.
- (3) Harvey, R. J., Depner, U. B., Wassle, H., Ahmadi, S., Heindl, C., Reinold, H., Smart, T. G., Harvey, K., Schutz, B., Abo-Salem, O. M., Zimmer, A., Poisbeau, P., Welzl, H., Wolfer, D. P., Betz, H., Zeilhofer, H. U., and Muller, U. (2004) *Science* 304, 884–887.
- (4) Manzke, T., Niebert, M., Koch, U. R., Caley, A., Vogelgesang, S., Hulsman, S., Ponimaskin, E., Muller, U., Smart, T. G., Harvey, R. J., and Richter, D. W. (2010) *J. Clin. Invest.* 120, 4118–4128.
- (5) Wang, H., Brozoski, T. J., Turner, J. G., Ling, L., Parrish, J. L., Hughes, L. F., and Caspary, D. M. (2009) *Neuroscience* 164, 747–759.
- (6) Unwin, N. (2005) *J. Mol. Biol.* 346, 967–989.
- (7) Kuhse, J., Laube, B., Magalei, D., and Betz, H. (1993) *Neuron* 11, 1049–1056.
- (8) Griffon, N., Buttner, C., Nicke, A., Kuhse, J., Schmalzing, G., and Betz, H. (1999) *EMBO J.* 18, 4711–4721.
- (9) Langosch, D., Thomas, L., and Betz, H. (1988) *Proc. Natl. Acad. Sci. U.S.A.* 85, 7394–7398.
- (10) Hoch, W., Betz, H., and Becker, C. M. (1989) *Neuron* 3, 339–348.
- (11) Burzomato, V., Groot-Kormelink, P. J., Sivilotti, L. G., and Beato, M. (2003) *Recept. Channels* 9, 353–361.
- (12) Grudzinska, J., Schemm, R., Haeger, S., Nicke, A., Schmalzing, G., Betz, H., and Laube, B. (2005) *Neuron* 45, 727–739.
- (13) Nicke, A., Rettinger, J., and Schmalzing, G. (2003) *Mol. Pharmacol.* 63, 243–252.
- (14) Zhou, Y., Nelson, M. E., Kuryatov, A., Choi, C., Cooper, J., and Lindstrom, J. (2003) *J. Neurosci.* 23, 9004–9015.
- (15) Groot-Kormelink, P. J., Broadbent, S. D., Boorman, J. P., and Sivilotti, L. G. (2004) *J. Gen. Physiol.* 123, 697–708.
- (16) Groot-Kormelink, P. J., Broadbent, S., Beato, M., and Sivilotti, L. G. (2006) *Mol. Pharmacol.* 69, 558–563.
- (17) Sigel, E., Kaur, K. H., Luscher, B. P., and Baur, R. (2009) *Biochem. Soc. Trans.* 37, 1338–1342.
- (18) Barrera, N. P., Herbert, P., Henderson, R. M., Martin, I. L., and Edwardson, J. M. (2005) *Proc. Natl. Acad. Sci. U.S.A.* 102, 12595–12600.
- (19) Barrera, N. P., Betts, J., You, H., Henderson, R. M., Martin, I. L., Dunn, S. M., and Edwardson, J. M. (2008) *Mol. Pharmacol.* 73, 960–967.
- (20) Shan, Q., Han, L., and Lynch, J. W. (2011) *PLoS One* 6, e28105.
- (21) Thompson, A. J., Price, K. L., and Lummis, S. C. (2011) *J. Physiol.* 589, 4243–4257.
- (22) Lochner, M., and Lummis, S. C. (2010) *Biophys. J.* 98, 1494–1502.